CIRCULATING COPY
Sent to Recall
In Two Weeks

UCID-20372

ELECTRICAL LINE SOURCE AND POINT SOURCE INTERACTIONS WITH ANOMALIES IN THE GROUND

R. J. Lytle
J. A. Beatty

December 1984

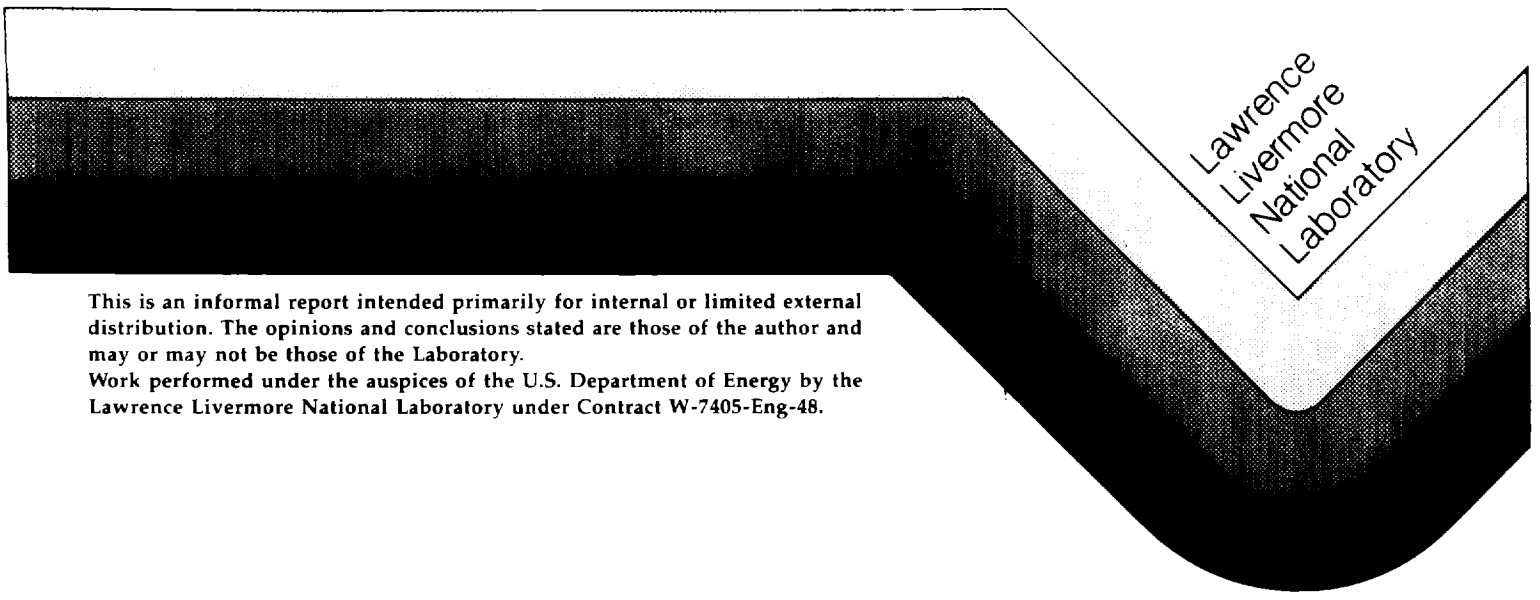

This is an informal report intended primarily for internal or limited external distribution. The opinions and conclusions stated are those of the author and may or may not be those of the Laboratory.
Work performed under the auspices of the U.S. Department of Energy by the Lawrence Livermore National Laboratory under Contract W-7405-Eng-48.

DISCLAIMER

This document was prepared as an account of work sponsored by an agency of the United States Government. Neither the United States Government nor the University of California nor any of their employees, makes any warranty, express or implied, or assumes any legal liability or responsibility for the accuracy, completeness, or usefulness of any information, apparatus, product, or process disclosed, or represents that its use would not infringe privately owned rights. Reference herein to any specific commercial products, process, or service by trade name, trademark, manufacturer, or otherwise, does not necessarily constitute or imply its endorsement, recommendation, or favoring by the United States Government or the University of California. The views and opinions of authors expressed herein do not necessarily state or reflect those of the United States Government or the University of California, and shall not be used for advertising or product endorsement purposes.

Printed in the United States of America
Available from
National Technical Information Service
U.S. Department of Commerce
5285 Port Royal Road
Springfield, VA 22161
Price: Printed Copy $ Microfiche $4.5

Page Range	Domestic Price	Page Range	Domestic Price
001-025	$ 7.00	326-350	$ 26.50
026-050	8.50	351-375	28.00
051-075	10.00	376-400	29.50
076-100	11.50	401-426	31.00
101-125	13.00	427-450	32.50
126-150	14.50	451-475	34.00
151-175	16.00	476-500	35.50
176-200	17.50	501-525	37.00
201-225	19.00	526-550	38.50
226-250	20.50	551-575	40.00
251-275	22.00	576-600	41.50
276-300	23.50	601-up[1]	
301-325	25.00		

[1]Add 1.50 for each additional 25 page increment, or portion thereof from 601 pages up.

ELECTRICAL LINE SOURCE AND POINT SOURCE INTERACTIONS WITH ANOMALIES IN THE GROUND

J. Lytle and J. Beatty

Lawrence Livermore National Laboratory

December 1984

ABSTRACT

Illustrative examples show that line source electrode interactions with a cylindrical anomaly can serve as an adequate qualitative model for point source electrode interactions with cylindrical and spherical anomalies. Subject to certain restrictions, the quantitative results for point and line source interactions with cylindrical anomalies can even be approximately the same. This is of benefit, due to the simplicity of the line source mathematical representation, in being able to determine the utility of means for sensing various anomalies within the ground.

1. INTRODUCTION

Electrical probing can be successfully used to detect spherical anomalies in the ground. Theoretical work has indicated in order for the anomaly to be detected, certain requisite conditions need to be met regarding the anomaly resistivity contrast to the host medium and the source/measurement electrode positions relative to the anomaly.[1-4]

In other ground probing studies, an anomaly of a different shape can be encountered. The requisite conditions pertinent to electrical probing about other anomalies need to be determined. This study addresses the considerations pertinent to a cylindrical anomaly.

It will be shown that the probing results for cylindrical and spherical anomalies can be roughly related to each other. Examples of these anomalies could include a mineral deposit, a hazardous-toxic waste leakage plume, an abandoned tunnel or a brine pocket near a prospective nuclear waste repository.

Some prior studies have concerned electrical detection of cylindrical anomalies.[2,5-7] Certain efforts have been concerned with line source and measurement electrodes located at the earth surface. A limited amount of study has been directed towards buried source and measurement electrodes. In this vein, to the author's knowledge, only one study[7] (an experimental study) exists providing any results illustrating the differences between point source and line source interactions with cylindrical anomalies. The comparisons given in this paper are theoretical and numerical results, rather than experimental comparisons.

Infinitely long line source and line measurement electrodes are never used in actual field work. They are only a mathematical convenience. For the line electrode approximation to be strictly valid, there necessarily should be: 1) no variations in ground electrical properties along the axis parallel to the line electrode, and 2) uniform current along the line electrode. The latter constraint means that end effects due to terminating the line should not be noticeable.

Field situations do not always satisfy these constraints. In addition, using line electrodes rather than point electrodes can require more complex field logistics. For these and other reasons, it is more common to use point electrodes rather than line electrodes in field work.

It is recognized that the spatial variation of fields about point electrodes is different than about line electrodes. Nevertheless, as others have noted,[1,6] the qualitative variation of electrical probing phenomena can be similar for analogous line and point electrode modeling results as long as: 1) there are primarily only two-dimensional variations in ground

electrical properties, 2) the point source/measurement electrode locations are positioned within a plane perpendicular to the two-dimensional ground structure, and 3) the separation between electrode locations and the anomalous ground features is not large. A large enough ensemble of field situations meet these criteria that line source modeling is worthwhile. As will be shown below, line source and point source probing results provide useful qualitative comparisons. In addition, if certain conditions are met, even quantitative results for electrical line electrodes and point electrodes can be quite close.

2. MATHEMATICAL MODELS

For reference purposes, the solution to Laplace's equation for a point source electrode and a line source electrode located exterior to a right circular cylinder anomaly. For the situation depicted in Fig. 1, the voltage due to a point source electrode[2] is

$$V = \frac{I}{4\pi\sigma_2 R} + \frac{I}{2\sigma_2 \pi^2} \int_0^\infty \sum_{m=0}^{\infty} \varepsilon_m \cos[m(\phi - \phi_s)] \cos[\lambda(z - z_s)] \cdot$$

$$\frac{(\frac{\sigma_2}{\sigma_1} - 1)\, I_m(\lambda a)\, K_m(\lambda \rho_s)\, I'_m(\lambda a)\, K_m(\lambda \rho)}{K_m(\lambda a) I'_m(\lambda a) - \frac{\sigma_2}{\sigma_1} I_m(\lambda a)\, K'_m(\lambda a)}\, d\lambda$$

for $\rho > a$ and

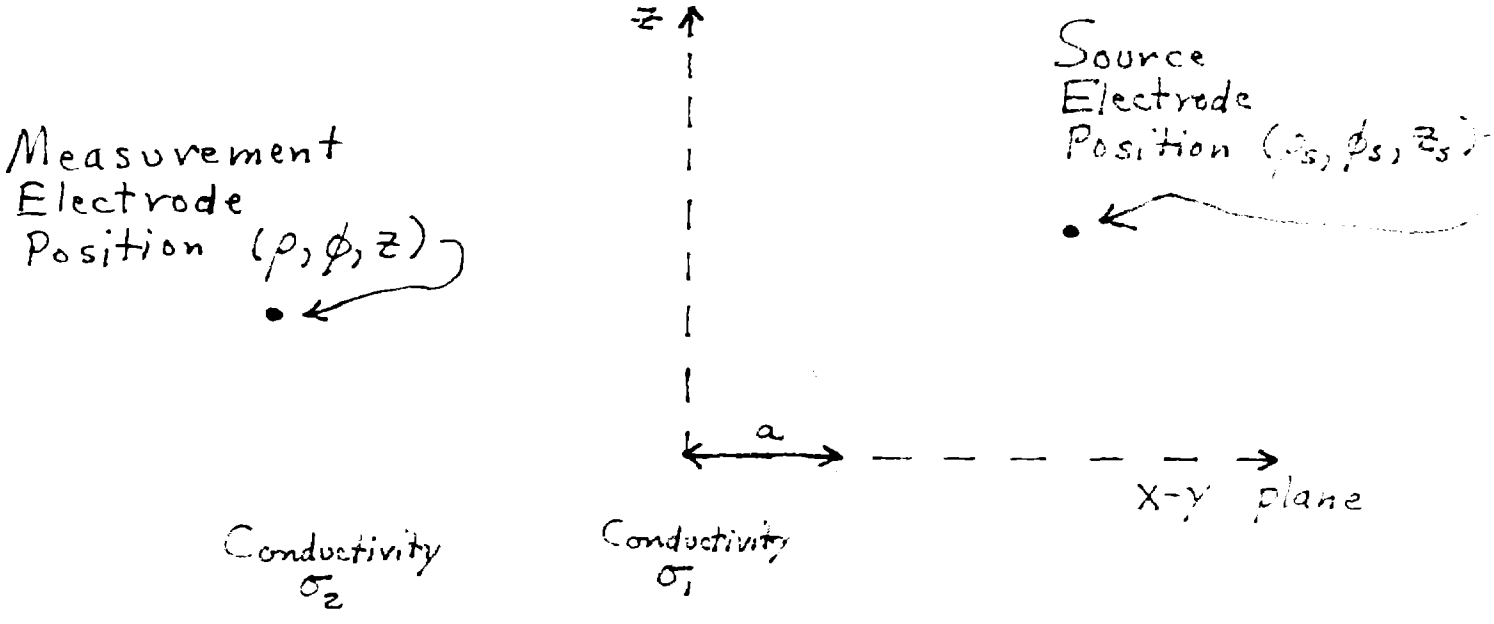

Figure 1. A right circular cylinder of radius a and conductivity σ_1 (resistivity ρ_1) is embedded in a homogeneous medium of conductivity σ_2 (resistivity ρ_2). A point source electrode and a point measurement electrode are shown. The cylindrical coordinate system is defined relative to the center of the cylindrical anomaly.

$$V = \frac{I}{2\sigma_1 \pi^2} \int_0^\infty \sum_{m=0}^{\infty} \varepsilon_m \cos[m(\phi - \phi_s)] \cos[\lambda(z - z_s)] \cdot$$

$$\frac{K_m(\lambda\rho_s)\, I_m(\lambda\rho)}{K_m(\lambda a) I'_m(\lambda a) - \frac{\sigma_2}{\sigma_1} I_m(\lambda a)\, K'_m(\lambda a)} \cdot \frac{1}{\lambda a}\, d\lambda$$

for $0 < \rho < a$.

In these expressions, the notation used for the right circular coordinate system is radius ρ, azimuthal angle ϕ and elevation z. R denotes the distance between the source and the measurement locations. The quantity ε_m is specified by $\varepsilon_0 = 1$ and $\varepsilon_m = 2$ for $m \geq 1$. The functions K_m and I_m are respectively the cylindrical Hankel and Bessel functions. The functions K'_m and I'_m are respectively the derivatives of K_m and I_m with respect to their argument.

For the situation shown in Fig. 2, the voltage due to a line source electrode[8] is

$$V = V_o + \frac{I}{2\pi\sigma_2} \frac{\sigma_2 - \sigma_1}{\sigma_2 + \sigma_1} \left[\ln \frac{1}{|\vec{\rho} - \vec{\xi}_s|} - \ln \frac{1}{|\vec{\rho}|}\right] + \frac{I}{2\pi\sigma_2} \ln \frac{1}{|\vec{\rho} - \vec{\rho}_s|} =$$

$$V_o + \frac{I}{2\pi\sigma_2} \frac{\sigma_2 - \sigma_1}{\sigma_2 + \sigma_1} \sum_{n=1}^{\infty} \frac{1}{n} \left(\frac{a^2}{\rho_s \rho}\right)^n \cos[n(\phi - \phi_s)] + \frac{I}{2\pi\sigma_2} \ln \frac{1}{|\vec{\rho} - \vec{\rho}_s|} \quad \text{for } \rho \geq a$$

and

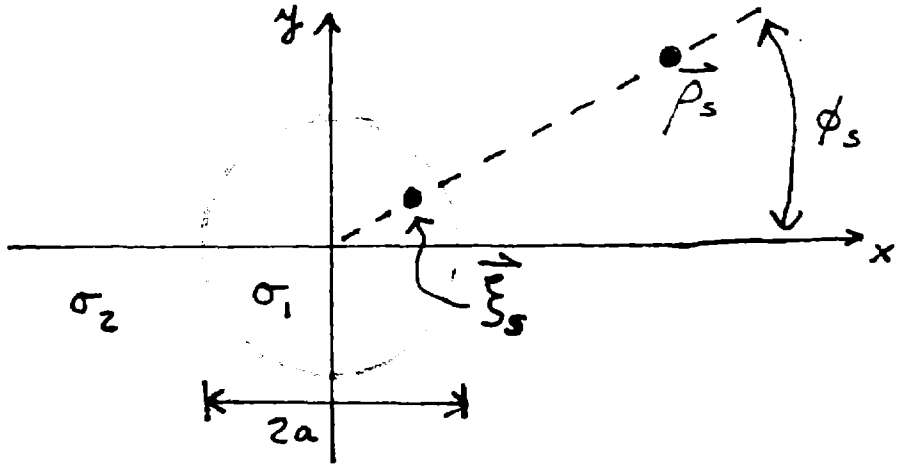

Figure 2. A line source of electrical current of amplitude I is at location $\vec{\rho}_s = (\rho_s, \phi_s)$ external to a right circular anomaly of radius a. The electrical conductivities internal and external to the cylinder are respectively σ_1 and σ_2. The measurement location $\vec{\rho}$ can be located internal or external to the cylinder. An "image" source located at position $\vec{\xi}_s = (\xi_s, \phi_s)$, where $\xi_s = a^2/\rho_s$ is useful in representing the field behavior.

$$V = V_0 + \frac{I}{\pi}\frac{1}{\sigma_2 + \sigma_1}\ln\frac{1}{|\vec{\rho} - \vec{\rho}_s|} - \frac{I}{2\pi\sigma_2}\frac{\sigma_2 - \sigma_1}{\sigma_2 + \sigma_1}\ln\frac{1}{|\vec{\rho}_s|}$$

$$= V_0 + \frac{I}{2\pi\sigma_2}\ln\frac{1}{|\vec{\rho}_s|} + \frac{I}{\pi\sigma_2}\frac{\sigma_2}{\sigma_2 + \sigma_1}\sum_{n=1}^{\infty}\frac{1}{n}\left(\frac{\rho}{\rho_s}\right)^n \cos[n(\phi - \phi_s)] \quad \text{for } 0 \leq \rho \leq a \ .$$

The definitions of the quantities $\vec{\rho}$ (the measurement location), $\vec{\rho}_s$ (the line source location), and $\vec{\xi}_s$ (the location of the image of the line source) are given in Fig. 2.

The quantity V_0 is a constant which is independent of position. Its value is dictated by boundary conditions. Most electrical probing involves two source electrodes of opposite voltage, hence the superposition of the effect due to two opposite sources is that the spatially constant potentials due to each cancel.

Comparisons of the electrical probing response for point and line sources exterior to a right circular cylindrical anomaly are needed to give a sound basis for the utility of using line electrodes in models rather than point electrodes. For convenience, it is assumed herein that both the point and line source interactions involve source locations, measurement locations, and cylindrical anomaly locations all remote from other electrical interfaces (such as the ground-air interface). The above formulas are suitable for describing such whole space interactions.

In many practical probing situations, either the source location, the measurement location, the anomaly location, or some combination of these may be in close proximity to the ground-air interface or some other interface with

an electrical contrast. For such situations, image theory can be readily used to define the appropriate whole-space problem approximating the half-space problem. It is worth mentioning that for a line source excitation, a rigorous solution to the half-space problem can be generated using a generalization of Parasnis' solution for electrodes at the ground surface.[5] The result would be the appropriate formulas expressed in terms of the bipolar coordinate system.

3. NUMERICAL MODELING RESULTS

Apparent resistivity probing results are respectively shown in Figs. 3 and 4 for point and line source interactions with a right circular cylindrical anomaly of conductivity $\sigma_1 = 0$ (e.g., an air-filled tunnel). These results represent four probe results for the source and measurement electrode positions indicated in the figures. The source electrodes are positioned within a borehole at $x = x_s$. The measurement electrodes are positioned within a borehole at $x = x_r$. The center of the source and measurement electrodes is varied in unison; i.e., $y_s = y_r$.

Note the close agreement between the corresponding apparent resistivity results for point source (Fig. 3) and line source (Fig. 4) interactions with this cylindrical anomaly. Figure 5 depicts the corresponding results for point electrodes interacting with a spherical anomaly of the same radius as the cylindrical anomaly. The qualitative comparison between the probing results for cylinders (Figs. 3 and 4) and for spheres (Fig. 5) is good. The quantitative correlation is somewhat surprisingly relatively close for point and line sources interacting with a cylinder (Figs. 3 and 4). The quantitative correlation is not, however, especially close for a cylindrical anomaly versus a spherical anomaly.

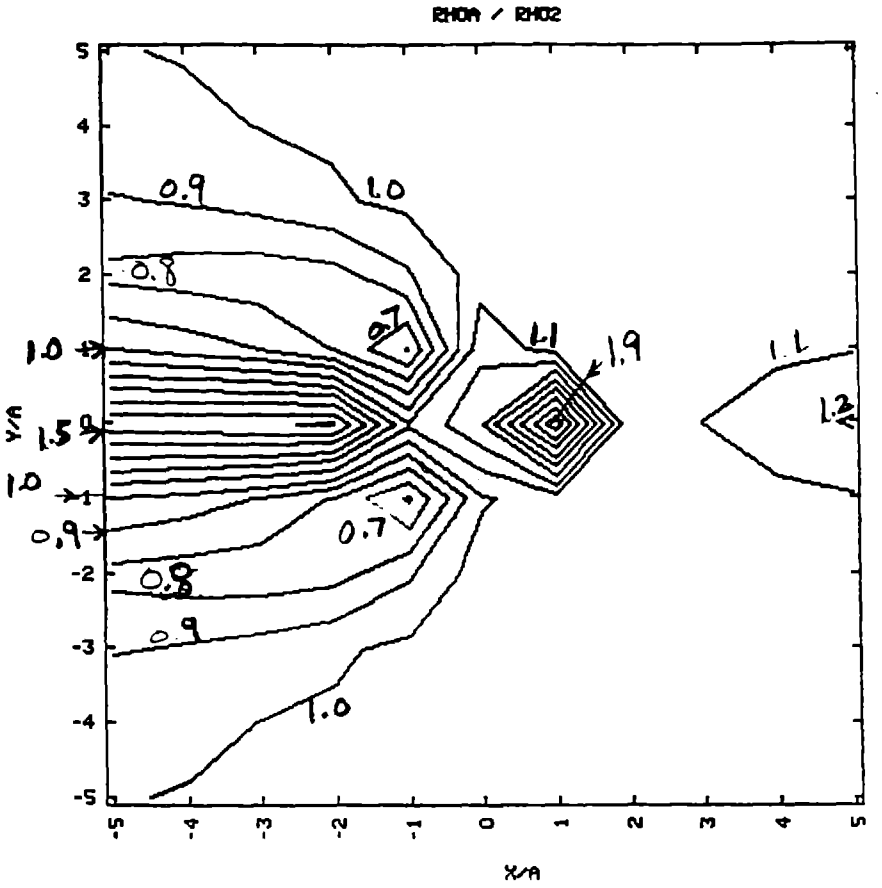

Figure 3a. $x_s = 1.5a$, $\sigma_1/\sigma_2 = 0$

Figure 3a. The results shown concern point electrode probing about an air-filled cylindrical anomaly. The ratio of the apparent resistivity to the resistivity of the host medium is plotted versus the center of the measurement electrode array. The source and measurement electrodes (each have two) are moved in unison with a common y position. The y offset between source electrodes is 0.2 a as is the y offset between the measurement electrodes. The source electrode array is constrained at the position $x_s = 1.5$ a.

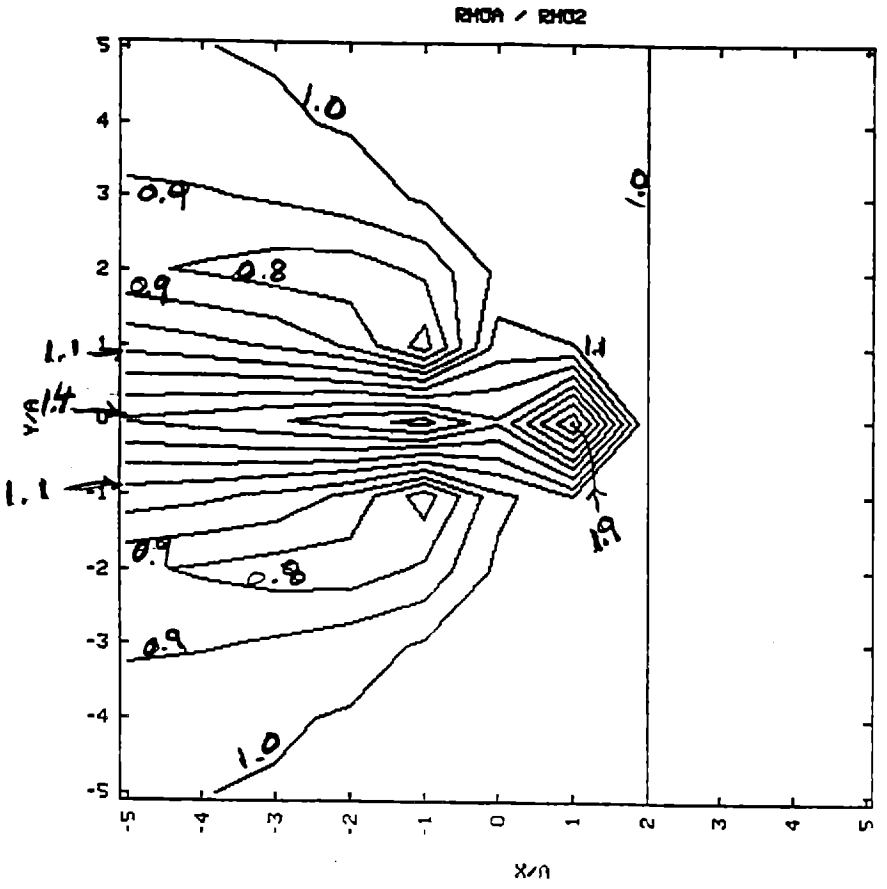

Figure 3b. $x_s = 2.0a$, $\sigma_1 / \sigma_2 = 0$

Figure 3b. The results shown concern point electrode probing about an air-filled cylindrical anomaly. The ratio of the apparent resistivity to the resistivity of the host medium is plotted versus the center of the measurement electrode array. The source and measurement electrodes (each have two) are moved in unison with a common y position. The y offset between source electrodes is 0.2 a as is the y offset between the measurement electrodes. The source electrode array is constrained at the position $x_s = 2.0$ a.

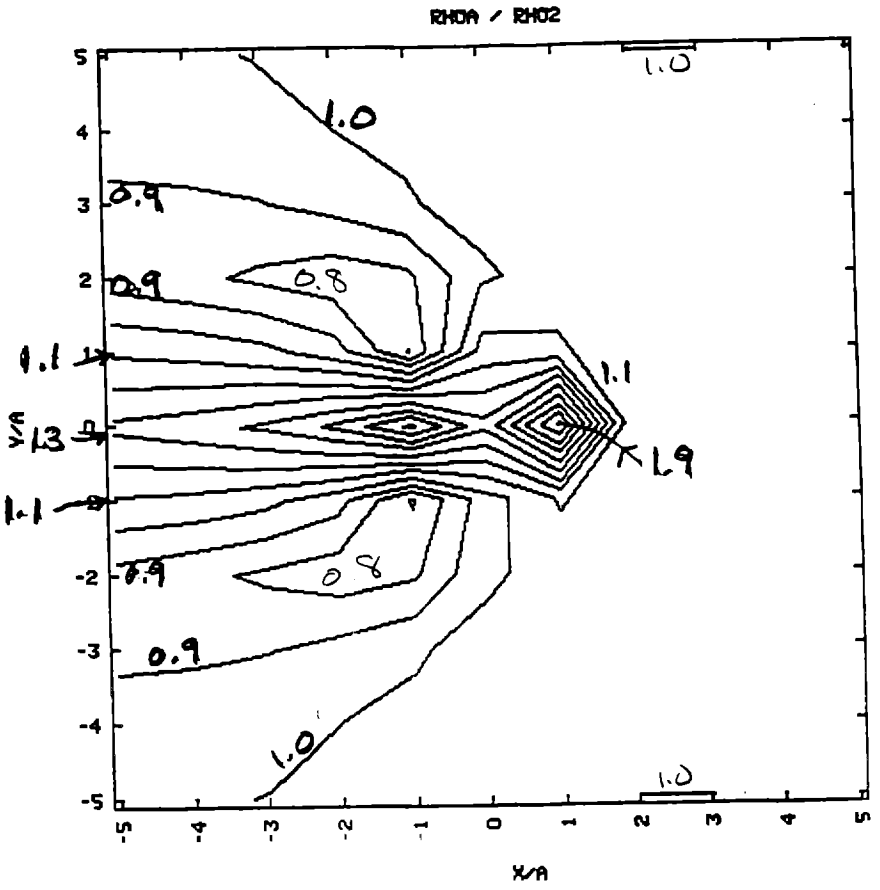

Figure 3c. $x_s = 2.5a$, $\sigma_1/\sigma_2 = 0$

Figure 3c. The results shown concern point electrode probing about an air-filled cylindrical anomaly. The ratio of the apparent resistivity to the resistivity of the host medium is plotted versus the center of the measurement electrode array. The source and measurement electrodes (each have two) are moved in unison with a common y position. The y offset between source electrodes is 0.2 a as is the y offset between the measurement electrodes. The source electrode array is constrained at the position $x_s = 2.5$ a.

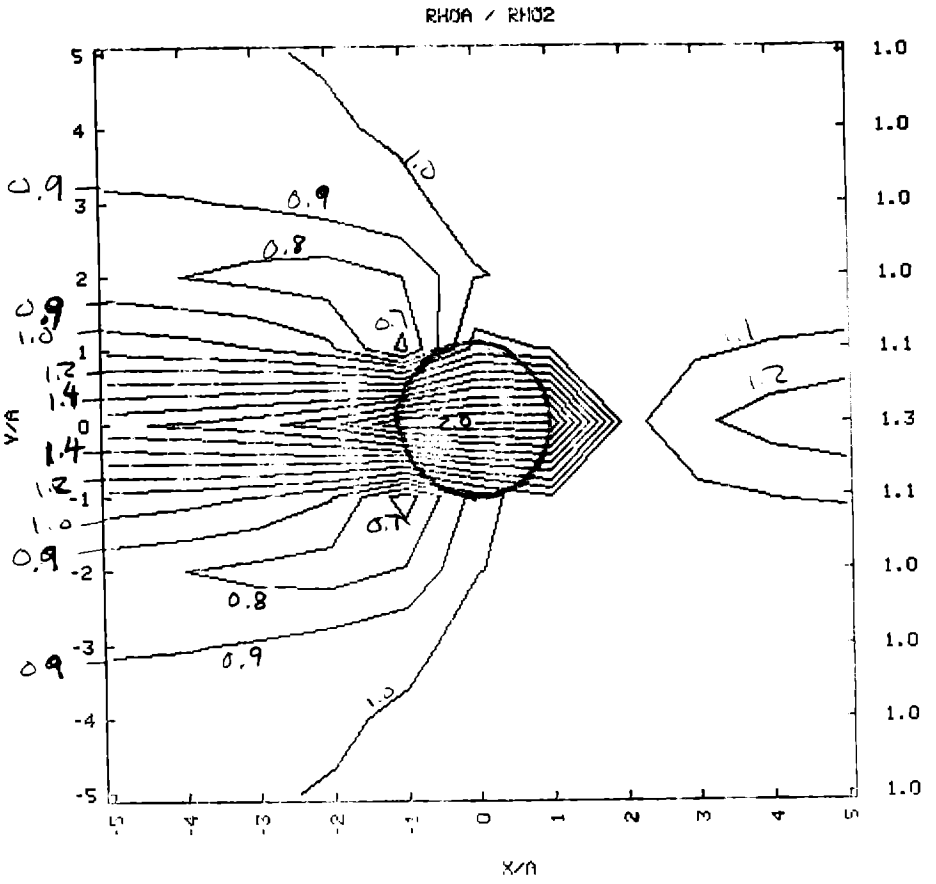

Figure 4a. $x_s = 1.5a$, σ_1/σ_2 -

Figure 4a. The results shown concern line electrode probing about an air-filled cylindrical anomaly. The ratio of the apparent resistivity to the resistivity of the host medium is plotted versus the center of the measurement electrode array. The source and measurement electrodes (each have two) are moved in unison with a common y position. The y offset between source electrodes is 0.2 a as is the y offset between the measurement electrodes. The source electrode array is constrained at the position $x_s = 1.5$ a.

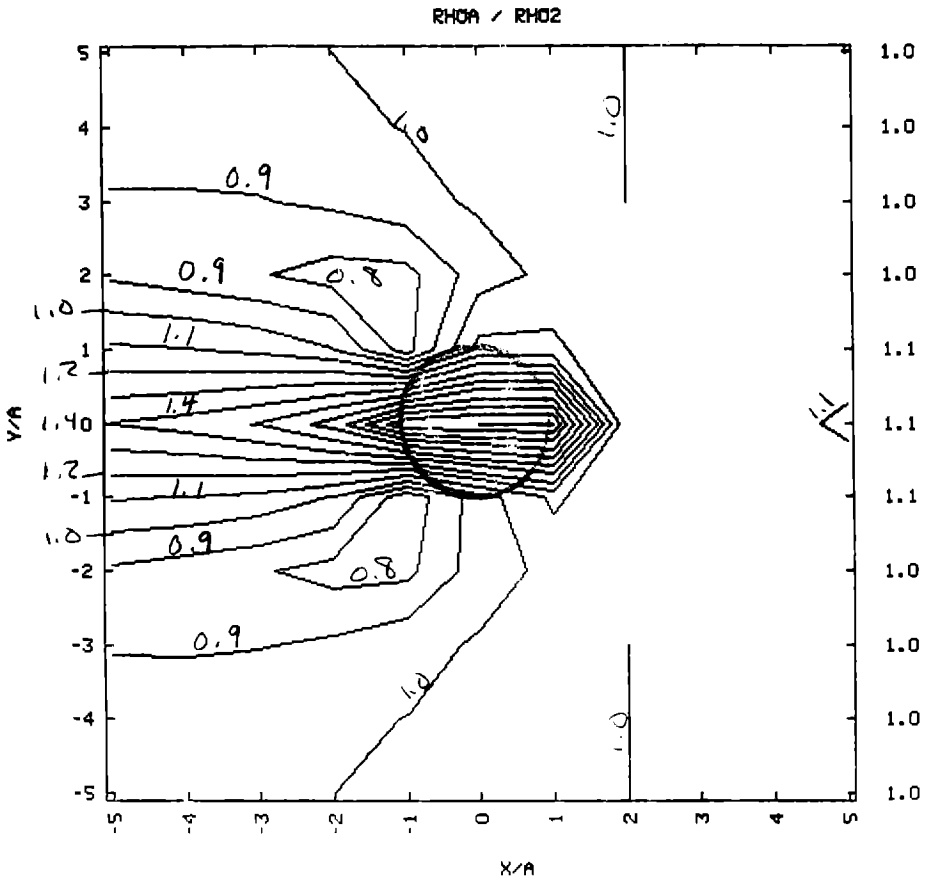

Figure 4b. $x_s = 2.0a$, $x_1 \; x_2 = 0$

Figure 4b. The results shown concern line electrode probing about an air-filled cylindrical anomaly. The ratio of the apparent resistivity to the resistivity of the host medium is plotted versus the center of the measurement electrode array. The source and measurement electrodes (each have two) are moved in unison with a common y position. The y offset between source electrodes is 0.2 a as is the y offset between the measurement electrodes. The source electrode array is constrained at the position $x_s = 2.0$ a.

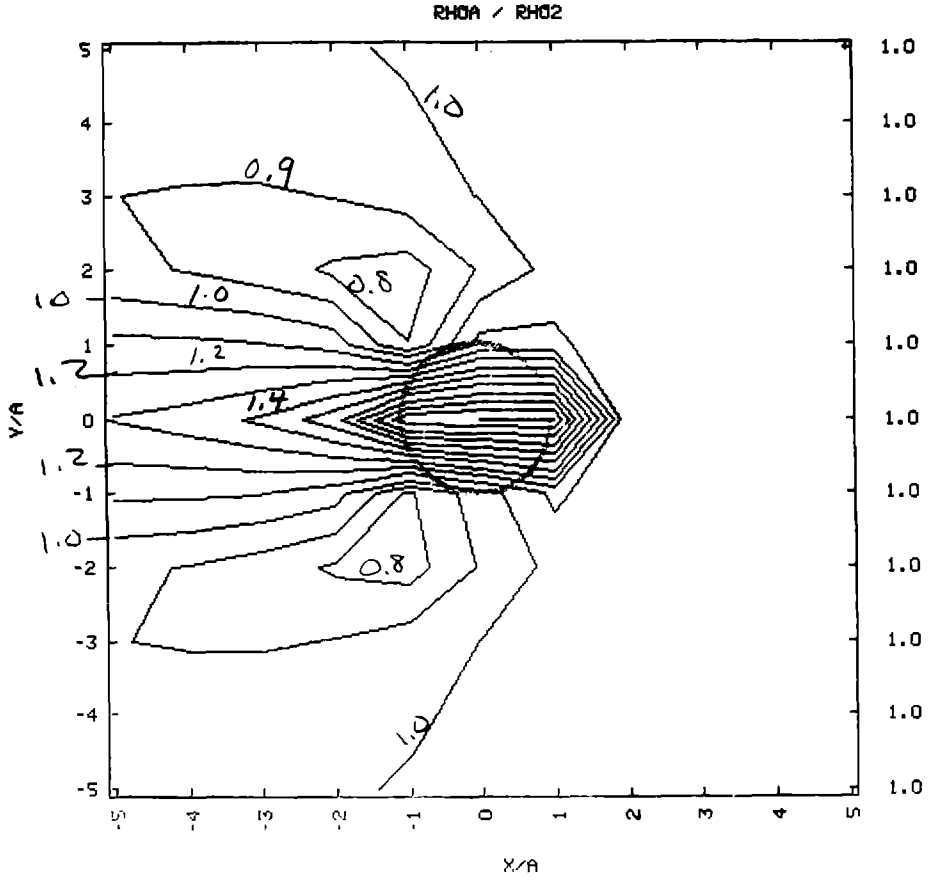

Figure 4c. $x_s = 2.5a$, $\sigma_1/\sigma_2 = 0$

Figure 4c. The results shown concern line electrode probing about an air-filled cylindrical anomaly. The ratio of the apparent resistivity to the resistivity of the host medium is plotted versus the center of the measurement electrode array. The source and measurement electrodes (each have two) are moved in unison with a common y position. The y offset between source electrodes is 0.2 a as is the y offset between the measurement electrodes. The source electrode array is constrained at the position $x_s = 2.5$ a.

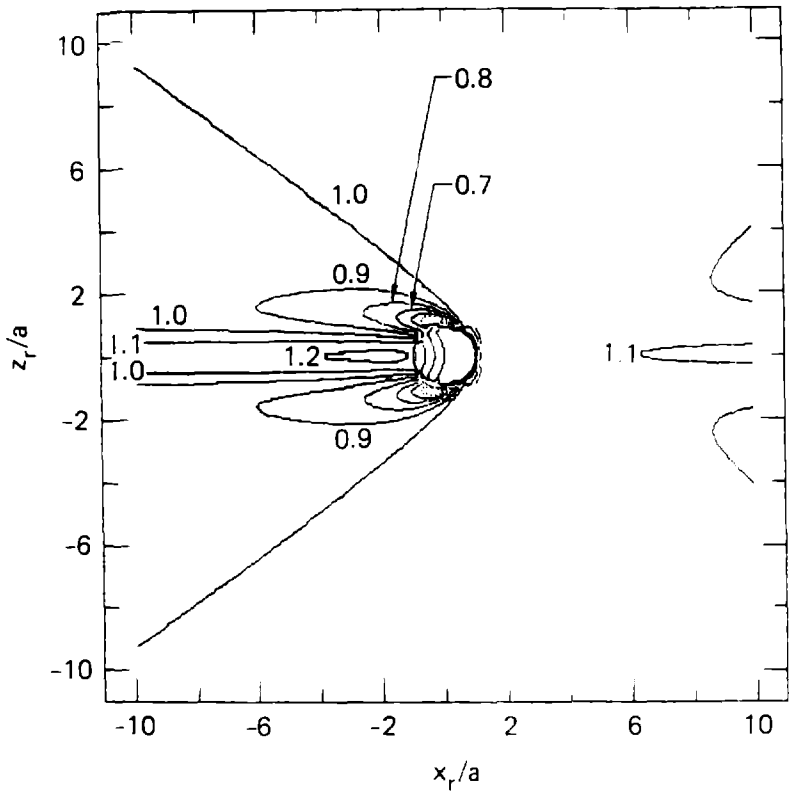

Figure 5a. $x_s = 1.5a$, $\sigma_1/\sigma_2 = 0$

Figure 5a. The results shown concern point electrode probing about an air-filled spherical anomaly. The ratio of the apparent resistivity to the resistivity of the host medium is plotted versus the center of the measurement electrode array. The source and measurement electrodes (each have two) are moved in unison with a common y position. The y offset between source electrodes is 0.2 a as is the y offset between the measurement electrodes. The source electrode array is constrained at the position $x_s = 1.5$ a.

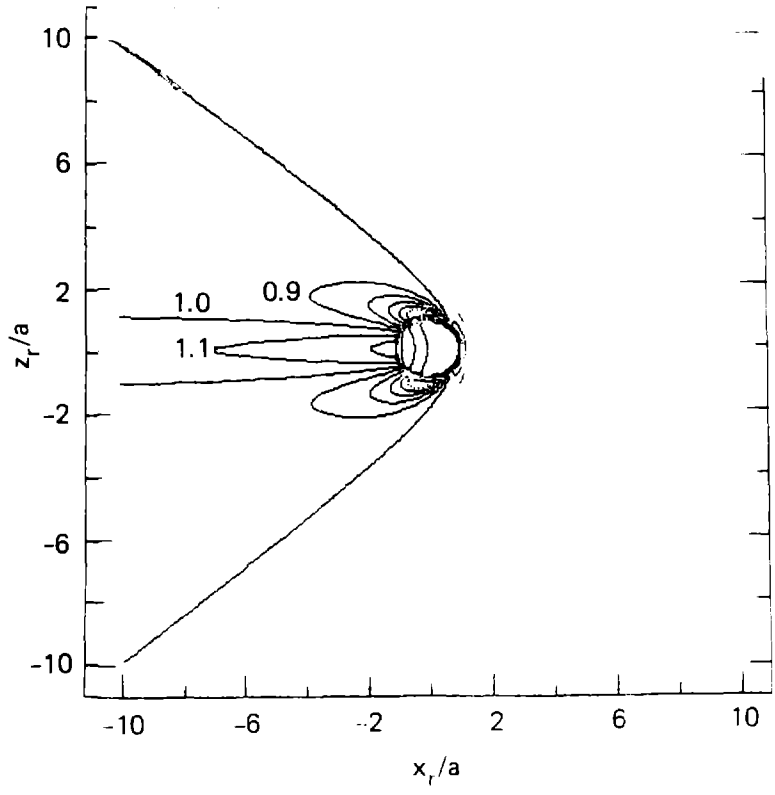

Figure 5b. $x_s = 2.0a$, $\sigma_1/\sigma_2 = 0$

Figure 5b. The results shown concern point electrode probing about an air-filled spherical anomaly. The ratio of the apparent resistivity to the resistivity of the host medium is plotted versus the center of the measurement electrode array. The source and measurement electrodes (each have two) are moved in unison with a common y position. The y offset between source electrodes is 0.2 a as is the y offset between the measurement electrodes. The source electrode array is constrained at the position $x_s = 2.0$ a.

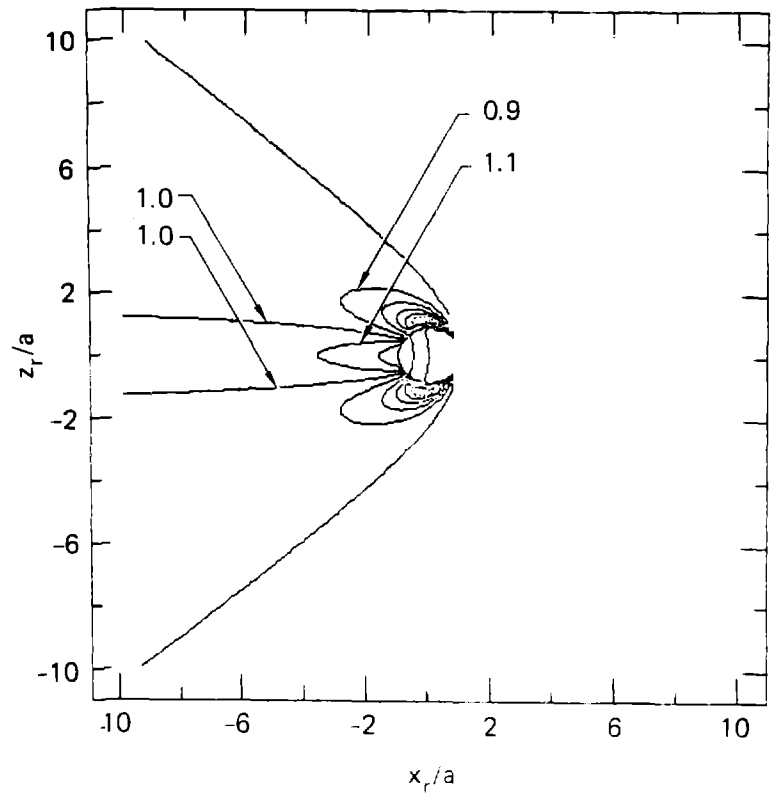

Figure 5c. $x_s = 2.5a$, $\sigma_1/\sigma_2 = 0$

Figure 5c. The results shown concern point electrode probing about an air-filled spherical anomaly. The ratio of the apparent resistivity to the resistivity of the host medium is plotted versus the center of the measurement electrode array. The source and measurement electrodes (each have two) are moved in unison with a common y position. The y offset between source electrodes is 0.2 a as is the y offset between the measurement electrodes. The source electrode array is constrained at the position $x_s = 2.5$ a.

To assess the validity of the numerical results for cylindrical anomalies, a simple scale model experiment was performed in a water tank with a long air-filled cylindrical anomaly. Although not shown here, a comparison of the numerical modeling and scale model results for point electrodes showed good agreement which lends credence to the point electrode numerical modeling procedure. The line electrode modeling is less complicated than the point electrode modeling and was, thus, not checked via an experiment.

For future reference purposes, four probe probing results for line sources interacting with a cylindrical anomaly are given in Figs. 6 and 7 with conductivity contrasts $\sigma_1/\sigma_2 = 0.1$ and 10.0. For the considerations that follow, the authors arbitrarily define an "observable" anomaly as one that has an apparent resistivity ρ_a deviating by 10 percent or more from the host medium.

A major conclusion evident from observing Figs. 3-7 is that for an anomaly of radius a, the anomaly is not "observable" unless either the source or observation electrodes is within a distance 3a of the center of the anomaly. If this constraint is met, then the other set of electrodes can be, in some cases, at distances of even up to 10a removed from the anomaly. Thus, detection over longer distances than might be intuitively obvious is feasible. The necessary constraint that one set of electrodes be relatively close to the anomaly, however, places a limit on the maximum probing distance useable if detectability of anomalies of radius a is required.

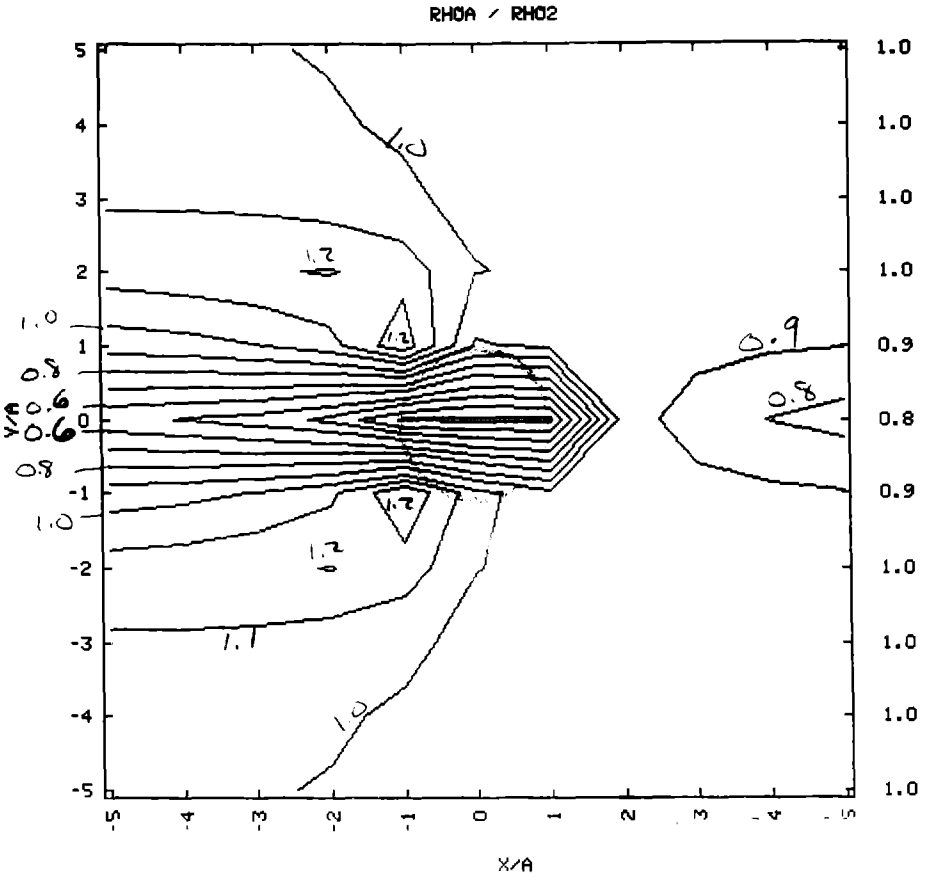

Figure 6a. x_s = 1.5a, σ_1/σ_2 = 10.0

Figure 6a. The results shown concern line electrode probing about a cylindrical anomaly. The ratio of the apparent resistivity to the resistivity of the host medium is plotted versus the center of the measurement electrode array. The source and measurement electrodes (each have two) are moved in unison with a common y position. The y offset between source electrodes is 0.2 a as is the y offset between the measurement electrodes. The source electrode array is constrained at the position x_s = 1.5 a. These results are for σ_1/σ_2 = 10.0.

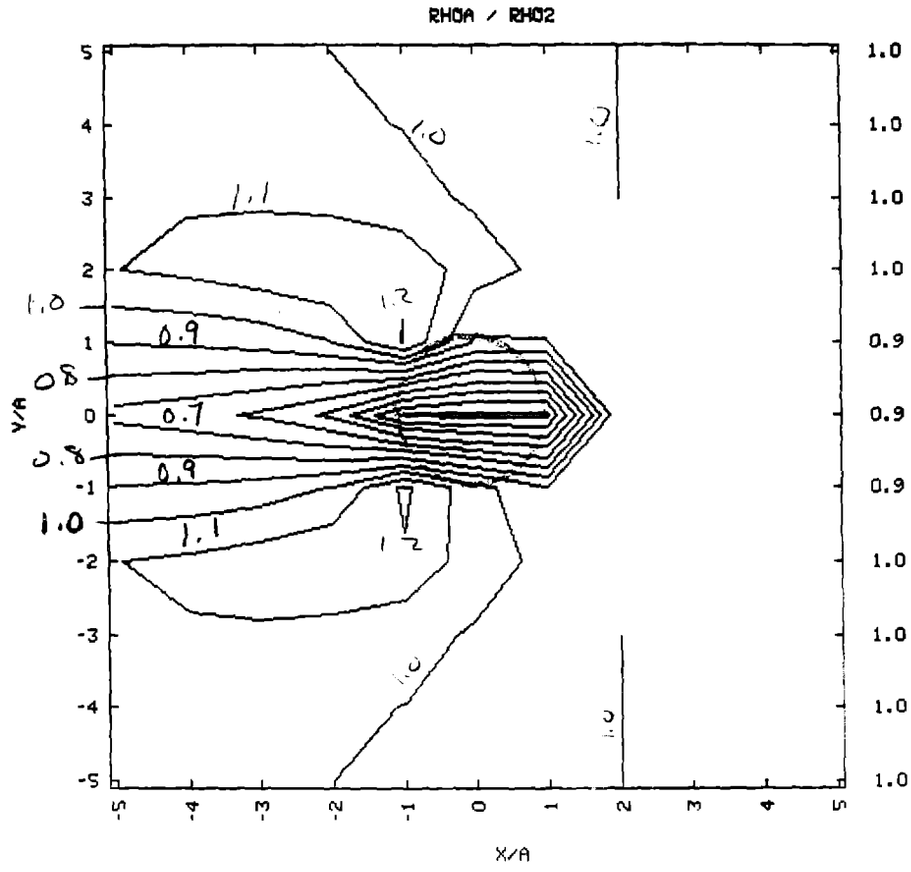

Figure 6b. $x_s = 2.0a$, $\sigma_1/\sigma_2 = 10.0$

Figure 6b. The results shown concern line electrode probing about a cylindrical anomaly. The ratio of the apparent resistivity to the resistivity of the host medium is plotted versus the center of the measurement electrode array. The source and measurement electrodes (each have two) are moved in unison with a common y position. The y offset between source electrodes is 0.2 a as is the y offset between the measurement electrodes. The source electrode array is constrained at the position $x_s = 2.0$ a. These results are for $\sigma_1/\sigma_2 = 10.0$.

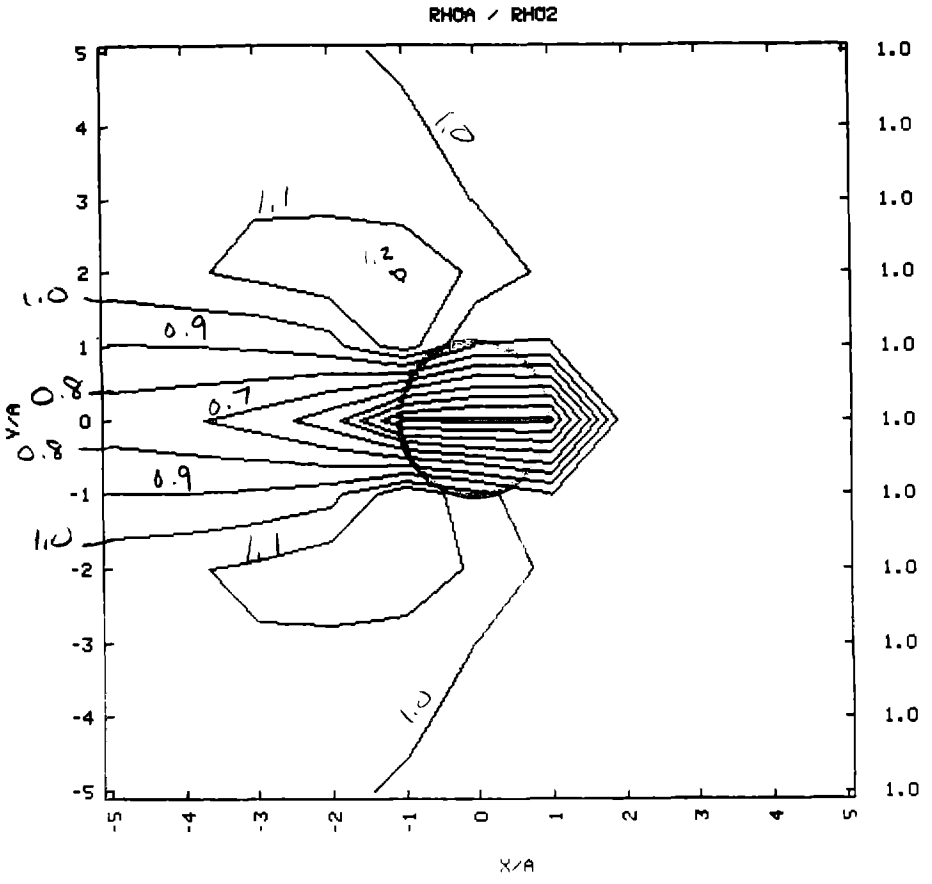

Figure 6c. x_s = 2.5a, σ_1/σ_2 = 10.0

Figure 6c. The results shown concern line electrode probing about a cylindrical anomaly. The ratio of the apparent resistivity to the resistivity of the host medium is plotted versus the center of the measurement electrode array. The source and measurement electrodes (each have two) are moved in unison with a common y position. The y offset between source electrodes is 0.2 a as is the y offset between the measurement electrodes. The source electrode array is constrained at the position x_s = 2.5 a. These results are for σ_1/σ_2 = 10.0.

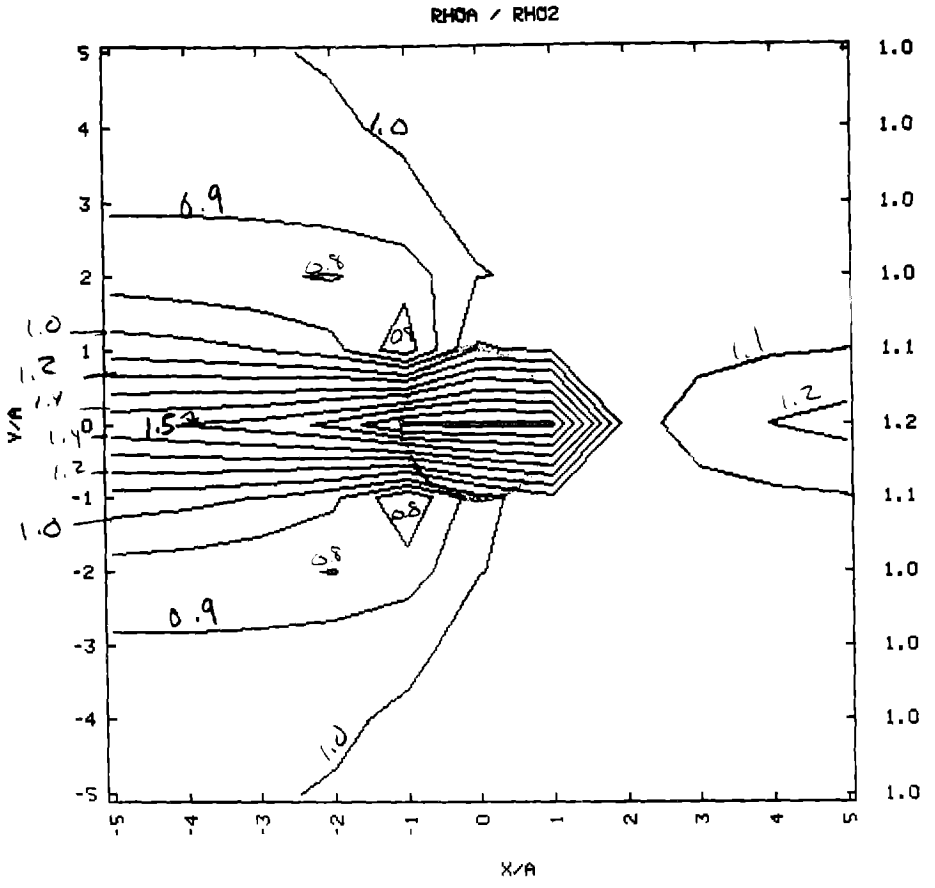

Figure 7a. $x_s = 1.5a$, $\sigma_1/\sigma_2 = 0.1$

Figure 7a. The results shown concern line electrode probing about a cylindrical anomaly. The ratio of the apparent resistivity to the resistivity of the host medium is plotted versus the center of the measurement electrode array. The source and measurement electrodes (each have two) are moved in unison with a common y position. The y offset between source electrodes is 0.2 a as is the y offset between the measurement electrodes. The source electrode array is constrained at the position $x_s = 1.5$ a. These results are for $\sigma_1/\sigma_2 = 0.10$. Note the close correspondence of these results with those of Fig. 4.

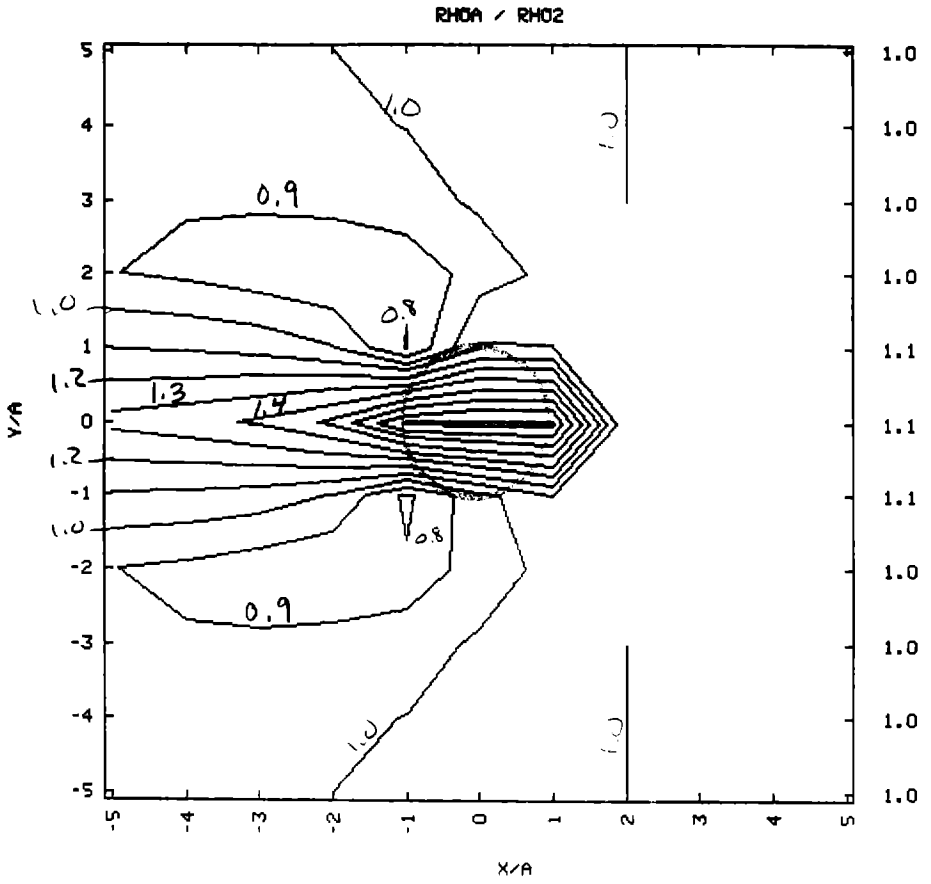

Figure 7b. $x_s = 2.0a$, $\sigma_1/\sigma_2 = 0.1$

Figure 7b. The results shown concern line electrode probing about a cylindrical anomaly. The ratio of the apparent resistivity to the resistivity of the host medium is plotted versus the center of the measurement electrode array. The source and measurement electrodes (each have two) are moved in unison with a common y position. The y offset between source electrodes is 0.2 a as is the y offset between the measurement electrodes. The source electrode array is constrained at the position $x_s = 2.0$ a. These results are for $\sigma_1/\sigma_2 = 0.10$. Note the close correspondence of these results with those of Fig. 4.

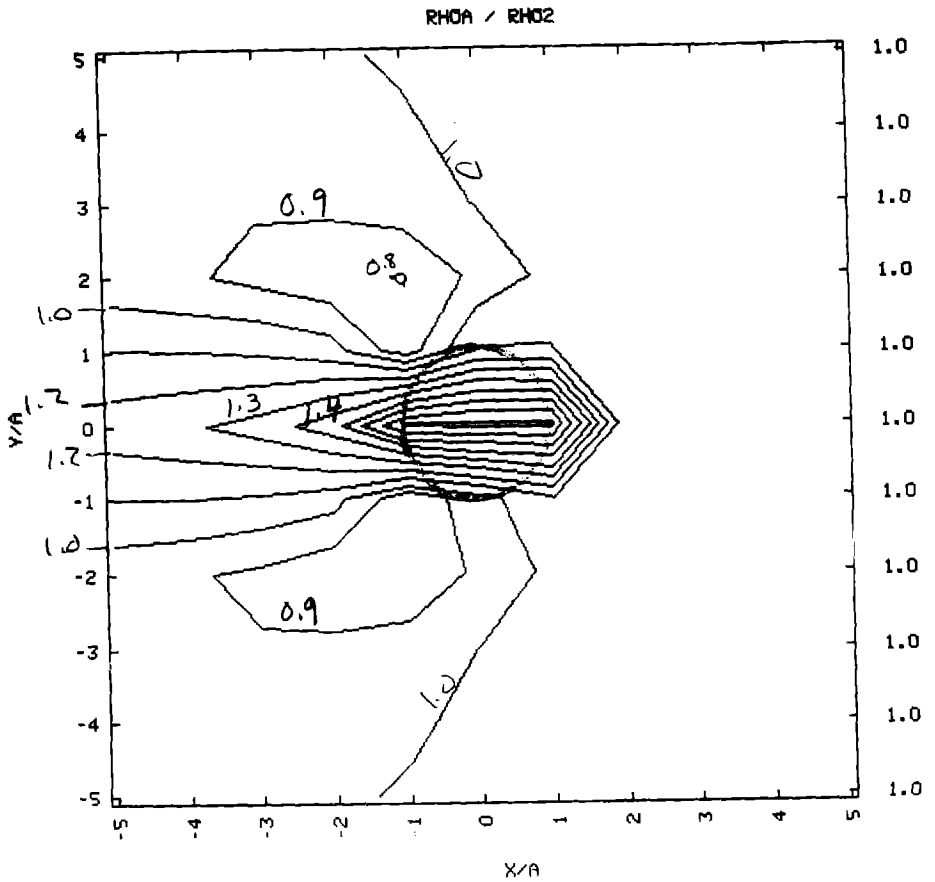

Figure 7c. $x_s = 2.5a$, $\sigma_1/\sigma_2 = 0.1$

Figure 7c. The results shown concern line electrode probing about a cylindrical anomaly. The ratio of the apparent resistivity to the resistivity of the host medium is plotted versus the center of the measurement electrode array. The source and measurement electrodes (each have two) are moved in unison with a common y position. The y offset between source electrodes is 0.2 a as is the y offset between the measurement electrodes. The source electrode array is constrained at the position $x_s = 2.5$ a. These results are for $\sigma_1/\sigma_2 = 0.10$. Note the close correspondence of these results with those of Fig. 4.

ACKNOWLEDGMENTS

The authors have benefited by conversations with Ed Laine and Abe Ramirez.

REFERENCES

1. R. G. Van Nostrand and K. L. Cook, Interpretation of Resistivity Data, U.S. Geological Survey Professional Paper 499, U.S. Government Printing Office, 1966 (see pp. 48-50 and 268-274).

2. J. R. Wait, Geo-Electromagnetism, Academic Press, 1982.

3. R. J. Lytle, Resistivity and Induced-Polarization Probing in the Vicinity of a Spherical Anomaly, IEEE Trans. on Geoscience and Remote Sensing, Vol. GE-20, No. 4, pp. 493- 499, October 1982.

4. R. J. Lytle and J. M. Hanson, Electrode Configuration Influence on Resistivity Probing with Vicinity of a Spherical Anomaly, Geophysics, Vol. 48, No. 8, pp. 1113-1119, August 1983.

5. D. S. Parasnis, Long horizontal cylindrical ore body at arbitrary depth in the field of two linear current electrodes, Geophysical Prospecting, 12, pp. 457-487, 1964.

6. I. R. Mufti, Finite-Difference Resistivity Modeling for Arbitrarily Shaped Two-Dimensional Structures, Geophysics, Vol. 41, No. 1, pp. 62-78, 1976.

7. H. Militzer, R. Roster-H. J. Brieden, Modellkurven Zum Geoelecktuschen Hohliaummachiveis-Electrodensysteme in Bohrlochen, Wissenschaftlichen Informations zentrums der Bergakademie, Freiberg, DDR, 1979.

8. P. M. Morse and H. Feshbach, Methods of Theoretical Physics, McGraw-Hill, pp. 1188-1189, 1953.